

## CHAPTER 1

# THE MOTT TRANSITION PROBLEM, DYNAMICAL MEAN FIELD THEORY, AND TRANSITION-METAL COMPOUNDS

GABRIEL KOTLIAR

Serin Physics Laboratory  
Rutgers University, Piscataway, NJ 08855-0849

### ABSTRACT

We review some aspects of the Mott transition from the point of view of dynamical mean-field theory, a generalization of the dynamical mean-field construction from classical to quantum systems. Comparison with experiments suggests that the approach captures some of the essential physics of three-dimensional transition-metal compounds. We conclude with directions for further extensions.

### 1.1 INTRODUCTION

The Mott transition [1], i.e. the interaction-driven metal-to-insulator transition, has many experimental realizations starting with the famous  $V_2O_3$  system. Recently these systems have been studied with much higher resolution and new compounds displaying similar physics have been synthesized [2].

From a theoretical point of view, this is a fundamental problem in the theory of strongly correlated electron systems which requires a coherent framework to describe the dual character of the electron: wave and particle, itinerant and localized. The two limits of well localized and fully itinerant are fairly well understood. In the weakly correlated limit, a wave-like description of the electron is appropriate. Fermi liquid theory explains why, at low energies, systems such as alkali metals behave as weakly interacting fermions. Their transport properties are well described by Boltzmann theory applied to long-lived quasiparticles, an approach that works well as long as  $k_F l \gg 1$ .

In insulators, far away from the Mott transition, the electron is well-described in real space. A solid is viewed as a regular array of atoms which bind an integer number of electrons. Transport occurs via activation, with the creation of vacancies and doubly-occupied sites. Atomic-physics calculations, together

with perturbation theory around the atomic limit, allows us to derive accurate spin Hamiltonians. The spectrum is composed of atomic excitations which are broadened to form states that have no single-particle character; these are known as Hubbard bands.

These two limits, well-separated atoms and strongly-overlapping bands, are easily described in real space and  $\mathbf{k}$ -space respectively. The strong correlation problem is the description of the electronic structure of solids away from these well-understood limits. The challenge is to develop new concepts and new computational methods, capable of describing situations where both itinerancy and localization are simultaneously important. The Mott transition problem forces us to confront these issues head-on.

Strongly correlated electron systems have anomalous properties resulting from the proximity to a localization delocalization boundary. We mention, among other things, resistivities that far exceed the Ioffe-Regel limit  $\rho_{Mott}^{-1} \approx e^2/hk_F$ , non-Drude like optical conductivities, and spectral functions that are not at all well-described by band theory [2]. To address this anomalous behavior one needs a technique capable of treating quasiparticle bands and Hubbard bands on the same footing, as well as providing a continuous interpolation between the atomic and band limits.

A recently developed approach to strongly correlated electron systems, the Dynamical Mean-Field Theory (DMFT), in the local-impurity self-consistent approximation, satisfies these requirements and has advanced our understanding of the Mott transition problem [3]. It is a great pleasure to present a contribution in the area of correlated electron systems in a conference in honor of P.W. Anderson. Phil introduced me to this problem when I was a graduate student. His early work permeates this entire subject and has been very influential in the developments I will present.

## 1.2 MODEL HAMILTONIAN

A minimal Hamiltonian to describe transition-metal oxides was introduced by P. W. Anderson in a classic paper. The electron moves via hopping integrals  $t_{ij}$  between localized states. The localizing influences are described by a matrix of on-site Coulomb interactions [4]. If the model is simplified further, by ignoring the orbital degeneracy, one obtains the Hamiltonian of the one-band Hubbard model

$$H = - \sum_{\langle ij \rangle, \sigma} (t_{ij} + \mu \delta_{ij}) (c_{i\sigma}^{\dagger} c_{j\sigma} + c_{j\sigma}^{\dagger} c_{i\sigma}) + U \sum_i n_{i\uparrow} n_{i\downarrow}, \quad (1.1)$$

which plays the role of the ‘‘Ising model’’ of strongly-correlated electrons. It is the simplest model describing the competition between localization and itinerancy.  $U$  is the Coulomb energy of two electrons occupying the same site,  $c_{i\sigma}^{\dagger}$ ,  $c_{j\sigma}$  are

creation and annihilation operators for an electron on a site  $i$ ,  $n_{i\sigma} = c_{i\sigma}^\dagger c_{i\sigma}$ , are the density of electrons at site  $i$  with spin  $\sigma = \uparrow, \downarrow$  [5].

The essential parameters in the model are the doping  $\delta$ , (or the chemical potential  $\mu$ ), the temperature  $T$ , and the ratio  $U/t$ . It turns out that the nature of the Mott transition depends on the degree of magnetic frustration in the insulating phase. The degree of magnetic frustration is thus another important parameter which is controlled by the lattice structure and the hopping integrals. Frustrated models are constructed, for example, by giving  $t$  and  $t'$  the nearest neighbors and next-nearest neighbors hopping amplitudes comparable values.

The solution of the Hamiltonian 1.1 has been a central problem in condensed matter physics, which has resisted exact solutions in more than one dimensions [6]. The opposite limit, of infinite lattice dimensionality was formulated by Metzner and Vollhardt. They pointed out that this limit is well defined if the hopping matrix elements are scaled [7] as  $t_{ij} = (\frac{1}{\sqrt{d}})^{|i-j|}$ , with  $|i-j|$  the minimum number of links that one has to traverse on the lattice in order to go between the points  $i$  and  $j$ , as  $d$  tends to infinity. In this limit the kinetic energy and the potential energy per site are of the same order retaining the main effects of the competition between the two terms.

Müller-Hartmann pointed out an essential simplification of the limit of large lattice coordination. While the Greens function depends on the wave vector via the Fourier transform of the hopping matrix elements,  $\epsilon_k$ , the self energy becomes  $k$  independent[8]:

$$G(k, i\omega_n) = \frac{1}{i\omega_n + \mu - \epsilon_k - \Sigma(i\omega_n)} \quad (1.2)$$

The one particle spectral function of the Hubbard in the limit of large lattice coordination then requires the computation of a function of one single variable, namely  $\Sigma(i\omega_n)$ . The limit of large lattice coordination was used to simplified several approximation schemes, such as perturbative expansions in the skeleton series [9], variational studies of the Gutzwiller type [10] Brandt and Mielsch [11]. used it to solve the the Falikov Kimball model a simplified version of the Hubbard model.

A different direction came about with the introduction of dynamical mean-field ideas which provided with a clear link between the Hubbard model, a model defined on a lattice, and the Anderson impurity model (AIM), a quantum impurity problem which had been introduced by P.W. Anderson nearly twenty years before, to describe magnetic moments in a metal [12]. In section 1.3 I present a pedagogical discussion of this connection which was done in collaboration with A.Georges [13]. For related work see refs [14]. Consequences of this insight to describe strongly correlated electron systems are described in the following sections. Phil's early work on the formation of local moments, greatly facilitated a direct solution of the Hubbard model in the limit of large lattice coordination,

which in turn gave rise to a deeper understanding of the correlation induced localization-delocalization transition.

### 1.3 MEAN FIELD THEORY OF CLASSICAL AND QUANTUM SYSTEMS

The goal of a mean-field theory is to approximate a lattice problem with many degrees of freedom by a *single-site effective problem*. The underlying physical idea is that the dynamics at a given site can be thought of as the interaction of the degrees of freedom at this site with an external bath created by all other degrees of freedom on other sites. We illustrate this idea with the Ising model with ferromagnetic couplings  $J_{ij} > 0$  between nearest-neighbor sites of a lattice with coordination  $z$ :

$$H = - \sum_{(ij)} J_{ij} S_i S_j - h \sum_i S_i \quad (1.3)$$

The Weiss mean-field theory views each given site (say,  $o$ ) as governed by an effective Hamiltonian:

$$H_{eff} = -h_{eff} S_o \quad (1.4)$$

Formally the effective Hamiltonian  $H_{eff}$  is obtained by performing a partial trace over all the spin variables except for the spin at site  $o$  in the partition factor

$$\frac{\int_{i \neq o} dS_i e^{-\beta H}}{\int_i dS_i e^{-\beta H}} \equiv e^{-H_{eff}[S_o]} \quad (1.5)$$

All the interactions with the other degrees of freedom are contained in the effective field  $h_{eff}$ :

$$h_{eff} = h + \sum_i J_{oi} m_i = h + zJm \quad (1.6)$$

where  $m_i = \langle S_i \rangle$  is the magnetization at site  $i$ , and translation invariance has been assumed ( $J_{ij} = J$  for n.n sites,  $m_i = m$ ). Hence  $h_{eff}$  has been related to a local quantity which can in turn be computed from the single-site effective model  $H_{eff}$ . For the simple case at hand, this reads:

$$m = \tanh(\beta h_{eff}) \quad (1.7)$$

which can be combined with (1.6) to yield the well-known mean-field equation for the magnetization:

$$m = \tanh(\beta h + z\beta Jm) \quad (1.8)$$

These mean-field equations are, in general, an approximation to the true solution of the Ising model. They become *exact* in the limit where the *coordination of the lattice becomes large*. It is quite intuitive indeed that the neighbors of a given site can be treated globally as an external bath when their number becomes large, and that the spatial fluctuations of the local field become negligible. As is clear from Eq. (1.6), the coupling  $J$  must be scaled as  $J = J^*/z$  to yield a sensible limit  $z \rightarrow \infty$  (this scaling ensures that both the entropy and the internal energy per site remain finite, so as to maintain a finite  $T_c$ ).

These ideas can be directly extended to quantum many-body systems and will be illustrated with the model Hamiltonian in eq. 1.1 [15] [3]. We assume that no symmetry breaking occurs, i.e. that one deals with the translation-invariant paramagnetic phase. The generalization to phases with broken symmetry is straightforward [3].

A mean-field description associates to the *lattice* Hamiltonian (1.1) a single-site effective dynamics, which is conveniently described in terms of an imaginary-time action for the fermionic degrees of freedom  $(c_{o\sigma}, c_{o\sigma}^+)$  at that site:

$$S_{eff} = - \int_0^\beta d\tau \int_0^\beta d\tau' \sum_\sigma c_{o\sigma}^+(\tau) \mathcal{G}_0^{-1}(\tau - \tau') c_{o\sigma}(\tau') + U \int_0^\beta d\tau n_{o\uparrow}(\tau) n_{o\downarrow}(\tau) \quad (1.9)$$

Formally we imagine integrating out all the degrees of freedom except for those living at that specific site in a path integral formulation. This step is the quantum analog of (1.5). The role of the effective local Hamiltonian  $H_{eff}$  is played by an effective local action  $S_{eff}$ .

The effects on the selected site of all the other sites which have been integrated out is contained in  $\mathcal{G}_0(\tau - \tau')$  which plays the role of the Weiss effective field. Its physical content is that of an effective amplitude for a fermion to be created on the isolated site at time  $\tau$  (coming from the "external bath") and being destroyed at time  $\tau'$  (going back to the bath). The main difference with the classical case is that this generalized "Weiss function" is a *function of time* instead of a single number. This, of course, is required to take into account *local quantum fluctuations*. Indeed, the mean-field theory presented here freezes spatial fluctuations but takes full account of local temporal fluctuations (hence the name 'dynamical').  $\mathcal{G}_0$  plays the role of a bare Green's function for the effective action  $S_{eff}$ , but it should not be confused with the non-interacting local Green's function of the original lattice model.

Notice that the knowledge of  $S_{eff}$  allows us to calculate *all the local* correlation functions of the original Hubbard model. A closed set of mean-field equations is obtained by supplementing Eq. (1.9) with the expression relating  $\mathcal{G}_0$  to local quantities computable from  $S_{eff}$  itself, in complete analogy with Eq. (1.6) above and reads:

$$\mathcal{G}_0(i\omega_n)^{-1} = i\omega_n + \mu + G(i\omega_n)^{-1} - R[G(i\omega_n)] \quad (1.10)$$

In this expression,  $G(i\omega_n)$  denotes the on-site interacting Green's function calculated from the effective action  $S_{eff}$ :

$$G(\tau - \tau') \equiv - \langle T c(\tau) c^\dagger(\tau') \rangle_{S_{eff}} \quad (1.11)$$

$$G(i\omega_n) = \int_0^\beta d\tau G(\tau) e^{i\omega_n \tau}, \quad \omega_n \equiv \frac{(2n+1)\pi}{\beta} \quad (1.12)$$

and  $R(G)$  is the reciprocal function of the Hilbert transform of the density of states corresponding to the lattice at hand. Explicitly, given the non-interacting density of states (d.o.s.)  $D(\epsilon)$  defined by  $D(\epsilon) = \sum_k \delta(\epsilon - \epsilon_k)$  with  $\epsilon_k \equiv \sum_{ij} t_{ij} e^{ik \cdot (R_i - R_j)}$ . The Hilbert transform  $\tilde{D}(\zeta)$  and its reciprocal function  $R$  are defined by:

$$\tilde{D}(\zeta) \equiv \int_{-\infty}^{+\infty} d\epsilon \frac{D(\epsilon)}{\zeta - \epsilon}, \quad R[\tilde{D}(\zeta)] = \zeta \quad (1.13)$$

For rigorous derivations of these equations the reader is refer to [15] [3]. Since  $G$  can in principle be computed as a functional of  $\mathcal{G}_0$  using the impurity action  $S_{eff}$ , Eqs (1.9,1.10,1.11) form a closed system of functional equations for the on-site Green's function  $G$  (analogous to the magnetization) and the Weiss function  $\mathcal{G}_0$  which contains the effects of the surrounding medium on the selected site. It is instructive to check these equations in two simple limits [13]:

- In the *non-interacting limit*  $U = 0$ , solving (1.9) yields  $G(i\omega_n) = \mathcal{G}_0(i\omega_n)$  and hence from (1.10),  $G(i\omega_n) = \tilde{D}(i\omega_n + \mu)$  reduces to the free on-site Green's function.
- In the *atomic limit*  $t_{ij} = 0$ , one just has a collection of disconnected sites and  $D(\epsilon)$  becomes a  $\delta$ -function, with  $\tilde{D}(\zeta) = 1/\zeta$ . Then (1.10) implies  $\mathcal{G}_0(i\omega_n)^{-1} = i\omega_n + \mu$  and the effective action  $S_{eff}$  becomes essentially local in time and describes a four-state Hamiltonian which yields:  $G(i\omega_n)_{at} = (1 - n/2)/(i\omega_n + \mu) + n/2(i\omega_n + \mu - U)$ , with  $n/2 = (e^{\beta\mu} + e^{\beta(2\mu-U)})/(1 + 2e^{\beta\mu} + e^{\beta(2\mu-U)})$ .

Solving the coupled equations above not only yields *local quantities* but also allows us to reconstruct all the  $\mathbf{k}$ -dependent correlation functions of the original lattice Hubbard model. For this purpose one needs to calculate the self energy from

$$\Sigma(i\omega_n) = \mathcal{G}_0^{-1}(i\omega_n) - G^{-1}(i\omega_n) \quad (1.14)$$

and substitute it in equation (1.2).

The dynamical mean-field equations can be studied on many different lattices. The lattice structure enters the single particle properties only via the density of states. There are many useful examples [3] but in the following we will focus on the Bethe lattice (Cayley tree) with coordination  $z \rightarrow \infty$  and nearest-neighbor hopping  $t_{ij} = t/\sqrt{z}$ . A semicircular d.o.s. is obtained in this case :

$$D(\epsilon) = \frac{1}{2\pi t^2} \sqrt{4t^2 - \epsilon^2} , \quad |\epsilon| < 2t \quad (1.15)$$

The Hilbert transform and its reciprocal function take very simple forms:

$$\tilde{D}(\zeta) = (\zeta - s\sqrt{\zeta^2 - 4t^2})/2t^2 , \quad R(G) = t^2 G + 1/G \quad (1.16)$$

so that the self-consistency relation between the Weiss function and the local Green's function takes in this case the explicit form:

$$\mathcal{G}_0^{-1}(i\omega_n) = i\omega_n + \mu - t^2 G(i\omega_n) \quad (1.17)$$

The same d.o.s. is also realized for a random Hubbard model on a fully connected lattice (all  $N$  sites pairwise connected) where the hoppings are independent random variables with variance  $t_{ij}^2 = t^2/N$ .

The structure of the dynamical mean-field theory is that of a functional equation for the local Green's function  $G(i\omega_n)$  and the 'Weiss function'  $\mathcal{G}_0(i\omega_n)$ . In contrast to the classical case, the on-site effective action  $S_{eff}$  remains a *many-body problem*. This is because the present approach freezes *spatial fluctuations* but fully retains *local quantum fluctuations*. As a function of imaginary time, each site undergoes transitions between the four possible quantum states  $|0\rangle$ ,  $|\uparrow\rangle$ ,  $|\downarrow\rangle$ ,  $|\uparrow, \downarrow\rangle$  by exchanging electrons with the rest of the lattice described as an external bath. The dynamics of these processes is encoded in the Weiss function  $\mathcal{G}_0(\tau - \tau')$ .

For these reasons, no Hamiltonian form involving *only* the on-site degrees of freedom ( $c_{o\sigma}, c_{o\sigma}^+$ ) can be found for the effective on-site model: once the bath has been eliminated,  $S_{eff}$  necessarily includes retardation effects. In order to gain physical intuition and also to make some practical calculations with  $S_{eff}$ , it is useful to have a Hamiltonian formulation [13]. This is possible upon reintroducing auxiliary degrees of freedom describing the 'bath'. For example, one can view ( $c_{o\sigma}, c_{o\sigma}^+$ ) as an 'impurity orbital', and the bath as a 'conduction band' described by operators ( $a_{l\sigma}, a_{l\sigma}^+$ ) and consider the Hamiltonian:

$$H_{AIM} = \sum_{l\sigma} \tilde{\epsilon}_l a_{l\sigma}^+ a_{l\sigma} + \sum_{l\sigma} V_l (a_{l\sigma}^+ c_{o\sigma} + c_{o\sigma}^+ a_{l\sigma}) - \mu \sum_{\sigma} c_{o\sigma}^+ c_{o\sigma} + U n_{o\uparrow} n_{o\downarrow} \quad (1.18)$$

This Hamiltonian is quadratic in  $a_{l\sigma}^+, a_{l\sigma}$ : integrating these out gives rise to an action of the form (1.9), with:

$$\mathcal{G}_0^{-1}(i\omega_n) = i\omega_n + \mu - \int_{-\infty}^{+\infty} d\omega \frac{\Delta(\omega)}{i\omega_n - \omega}, \quad \Delta(\omega) \equiv \sum_{l\sigma} V_l^2 \delta(\omega - \tilde{\epsilon}_l) \quad (1.19)$$

Hence Eq. (1.18) can be viewed as a Hamiltonian representation of  $S_{eff}$  provided the  $\Delta(\omega)$  (i.e the parameters  $V_l, \tilde{\epsilon}_l$ ) is chosen such as to reproduce the actual solution  $\mathcal{G}_0$  of the mean-field equations. The spectral representation Eq. (1.19) is general enough to permit this in all cases. Note that the  $\tilde{\epsilon}_l$ 's are *effective* parameters that should not be confused with the single-particle energies  $\epsilon_k$  of the original lattice model. The Hamiltonian (1.18) is the Anderson model of a magnetic impurity coupled to a conduction bath [12]. Note however that the shape of the hybridization function  $\Delta(\omega)$  is *not known a priori* in the present context but must be found by solving the self-consistent problem. The isolated site  $o$  plays the role of the impurity orbital, and the conduction bath is built out of all other sites. Comparing eq. 1.19 with 1.17 allows us to rewrite the mean-field equations in terms of the hybridization function now written as a function of Matsubara frequencies  $\Delta(i\omega_n) \equiv \sum_l \frac{V_l^2}{(i\omega_n - \tilde{\epsilon}_l)}$

$$t^2 G_{imp}(i\omega_n)[\Delta, \alpha] = \Delta(i\omega_n). \quad (1.20)$$

The index  $\alpha$  denotes all the parameters of the problem such as  $T, U$  etc. The quantity  $G_{imp}$  is the local Greens function of the Anderson impurity model.

The reduction of a lattice problem to a single-site problem with *effective* parameters is a common feature of both the classical and the quantum mean-field constructions. The main difference is that the Weiss field is a number in the classical case, and a function in the quantum case. Physically, this reflects the existence of *many energy scales* in strongly correlated fermion models. (We note in passing that this also occurs in the mean-field theory of some classical problems with many energy scales such as spin glasses). This points out to the limitations of other ‘mean-field’ approaches, such as the Hartree-Fock approximation or slave bosons methods, where one attempts to parametrize the whole mean-field function by a single *number* (or a few of them). This in effect amounts to freezing local quantum fluctuations by replacing the problem with a purely classical one, and can only be reasonable when a single low-energy scale is important. This is the case for instance for a Fermi liquid phase. However, even in such cases, parametrizing the Weiss field by a single number can only be satisfactory at low energy, and misses the high energy incoherent features associated with the other energy scales in the problem. When no characteristic low-energy scale is present, a single number parametrization fails completely.

Finally, besides its intuitive appeal, the mapping onto impurity models has proven to be useful for two reasons. First, it allows us to understand qualitatively the physics of the Hubbard model in the limit of large lattice coordination by

exploiting the known analytic structure of the Anderson impurity model. The key insight is that the impurity model is generally an analytic function of the interaction  $U$ . Hence, all the non-analyticities in the problem result from the self-consistency condition Eq. (1.20). Second, the Anderson impurity model can be accurately solved with a variety of techniques[16], which in combination with the self consistency conditions such as 1.20, resulted in a quantitative solution of many models of lattice correlated electrons [3].

#### 1.4 SPECTRAL FUNCTIONS AND LOCAL VIEW OF STRONGLY CORRELATED STATES

A simple local picture of the various regimes of the Hubbard model follows from the early work of Anderson and Yuval, and Anderson Yuval and Hamman [17]. Their results are instrumental for generating the qualitative picture of the spectra of the Hubbard model in large dimensions [13]. They propose to express the partition function of the Anderson impurity model as a sum over histories of the local-impurity spin as is currently done in the modern computer evaluations of the partition function using the Hirsch Fye algorithm [18]. Then, the partition function is expressed in terms of the positions of the spin flips or kinks in the spin impurity history.

In the DMFT context those kinks represent the transitions between the degenerate ground states of the paramagnetic phase of the Mott insulator, i.e. *local* spin fluctuations.

$$Z = \sum_n \sum_{\tau_1 \dots \tau_n} y_1 \dots y_n e^{-A[\tau_1 \dots \tau_n]}. \quad (1.21)$$

The  $y_i$ 's in eq. (1.21) are the Anderson-Yuval fugacities for flipping the spin, and  $A$  is the action that governs the interactions among the kinks, i.e. the energy of the fermionic degrees of freedom in the presence of a sequence of spin flips at times  $\tau_1 \dots \tau_n$ . It results from integrating out the bath electrons that hybridize with the impurity.

When the system is metallic, the bath function has finite density of states at low energies [ $\Delta(i\omega_n) \propto -i \text{sign}(\omega_n)$ ]. The interaction between the spin flips is logarithmic, and the number of spin flips proliferates at long times (low energies). The local spin-spin autocorrelation function then decays as  $\frac{1}{\tau^2}$  at long times.

On the other hand, in the Mott insulating state, the self-consistent hybridization function has zero density-of-states at low frequencies [ $\Delta(i\omega_n) \propto -i \omega_n$ ]. This gives rise to a confining interaction among the kinks since now  $\mathcal{G}_0$  does not decay. The local impurity spin now has long-range order in time. In this case, the interaction between the Fermions and the spin fluctuations remains finite at low frequencies. A gap opens in the one-particle excitation spectrum.

The mapping onto an Anderson impurity model offers an intuitive picture of both metallic states and Mott insulating states. A correlated metal is described

locally as an Anderson impurity model in a metallic bath: The Kondo effect gives rise to strongly renormalized quasiparticles when the interactions are strong, and to a broad band when the interactions are weak. A Mott insulator is locally described as an Anderson impurity model in an insulating bath. The charge degrees of freedom are gapped, but the spin degrees of freedom are not quenched; they dominate the low-energy physics. When there is one electron per site, the Mott transition takes place as one goes from the first regime to the second by increasing the strength of the interaction  $U$  [19].

A sketch of the evolution of the spectral function  $-ImG(i\Omega + i\delta)$  of the half filled Hubbard model is described in figure (1.1). For interactions  $U$  close but smaller than the critical  $U_{c2}$  the one-electron spectral function of the Hubbard model in the strongly correlated metallic region contains both atomic features (i.e. Hubbard bands) and quasiparticle features in its spectra [13]. This may be understood intuitively from the Anderson-Yuval-Hamman path-integral representation. In the regime of strong correlations, paths that are nearly constant in imaginary time, as well as those that fluctuate strongly, have substantial weight in the path integral [17]. The former give rise to the Hubbard bands, while the latter are responsible for the low-frequency Kondo resonance. Two features in this spectra are surprising. First the narrow central peak before the Mott transition, resulting from quasiparticle states formed in the background of the coherent Kondo tunneling of the local spin fluctuations. Second atomic physics leaves a signature on the one particle spectral properties in the form of well formed Hubbard at higher frequency, in the strongly correlated metallic state.

As the transition at zero temperature is approached, there is a substantial transfer of spectral weight from the low-lying quasiparticles to the Hubbard bands. The Mott transition at zero temperature takes place at a critical value of  $U$ , denoted by  $U_{c2}$  where the integrated spectral weight at low frequency vanishes, as shown in figure 1.1. This results in a Mott transition point where the quasiparticle mass diverges, but a discontinuous gap opens in the quasiparticle spectra [20]. These results are in agreement with the early work of Fujimori *et al.* [21], who arrived at essentially the same picture on the basis of experiment. It is worth remarking that the spectral function in the strongly correlated metallic region is better regarded as composed of three components: Hubbard bands centered at  $U/2$ , a low-energy quasiparticle peak with a height of order unity and a total intensity proportional to  $(U_{c2} - U)$  distributed over an energy range  $U_{c2} - U$ , and an incoherent background connecting the high energy to the low energy region. The last feature ensures that there is no real gap between the quasiparticle features and the Hubbard bands, as long as one stays in the metallic regime. The intensity in the background between the quasiparticles and the Hubbard bands can be estimated to vanish as  $(U_{c2} - U)^{1/2}$ .

The Anderson Yuval Coulomb gas was extended to the study of the mixed valence by Haldane [22]. The local configurations contain low lying charge and spin fluctuations. Surprisingly the mixed valence regime occurs in a wide region

#### 1.4. SPECTRAL FUNCTIONS AND LOCAL VIEW OF STRONGLY CORRELATED STATES 11

of parameters when the Anderson impurity model describes the local physics of a lattice system [23]. A general extended Hubbard model [24] was investigated extensively using the Anderson Yuval Coulomb gas approach. There is a regime of parameters where the charge fluctuations are *incoherent*. In this regime the physics is similar to that of the Falikov Kimball [25] model. The physics is described Fermions which are strongly scattered off quasiclassical low energy local modes which cannot tunnel coherently between the degenerate states, and instead flip among them incoherently [23][24]. Systems of this kind, Falikov Kimball liquids, are accurately described by Hubbard III like approximations, which are now viewed in a new light as accurate solutions of the dynamical mean-field equations in a regime where the Coulomb gas fugacities remain small. The Hubbard III approximation, describes very low lying local spin fluctuations in a regime where they are not quenched by the fermionic degrees of freedom. Other charge or orbital fluctuations can play the role of the spin fluctuation in more complex (multiorbital) systems. The coupling of these unquenched collective modes to quasiparticles gives rise to the incoherent regime.

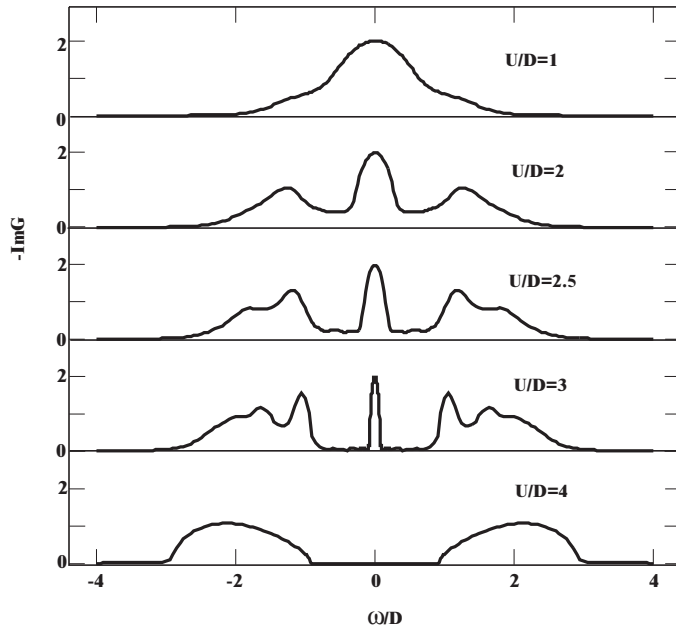


Figure 1.1: Evolution of the spectral function at zero temperature as function of  $U$ . From Ref. [20].

## 1.5 ANOMALOUS RESISTIVITY AND TRANSFER OF SPECTRAL WEIGHT

The results described in the previous section require a large degree of magnetic frustration to suppress the long-range order and to stabilize a finite temperature paramagnetic insulator with finite entropy. In systems without magnetic frustration, the onset of magnetism prevents us from accessing the strongly correlated regime. Indeed in the absence of frustration the quasiparticle residue in the antiferromagnetic metal to antiferromagnetic insulator transition remains finite, while it is vanishingly small in the paramagnetic metal to paramagnetic insulator transition [26].

However in three dimensional transition metal oxides [27] orbital degeneracy introduces magnetic frustration weakening the strength of magnetic correlations enough to make the strongly correlated regime observable. This can be understood in very simple physical terms, exchange among identical orbitals is antiferromagnetic while exchange among orthogonal orbitals has ferromagnetic character. In the absence of orbital ordering, cancellation between these two processes takes place resulting in reduction of the magnetic interactions between neighboring spins.

The phase diagram of a *partially frustrated* Hubbard model is shown in fig.(1.2). This dynamical mean-field phase diagram has the same topology as the observed phase diagram of  $V_2O_3$  and  $NiSe_{2-x}S_x$  [2]. In such cases, the change from the paramagnetic insulator (localized) to the paramagnetic metal (extended) regime occurs, as a function of  $U/t$ , as a first-order phase transition [28, 29].

There is a remarkable degree of universality in the high temperature part of the phase diagram describing the localization delocalization phase transition (below  $T_c$ ) and the localization delocalization crossover (above  $T_c$ ) which follows from the Landau analysis discussed in the next section. This phase diagram is *generic*, while concrete calculations have been performed mostly for the one-band model, the first-order phase transition takes place for arbitrary orbital degeneracy, as long as magnetic order is sufficiently suppressed. The basic physical ingredients for obtaining such a first order line are on site repulsion comparable than the bandwidth and magnetic frustration to suppress the onset of magnetic long range order.

The phase diagram in Fig. 1.2 displays two crossover lines. The dotted line is a coherence-to-incoherence crossover (i.e. the continuation of the  $U_{c2}$  line where metallicity is lost). The shaded area is a continuation of the  $U_{c1}$  line, where the temperature becomes comparable with the gap. Figure 1.3 describes the anomalous resistivities near the crossover region. They are qualitatively similar to the behavior of the resistivity of  $V_2O_3$  and in the  $NiSe_{2-x}S_x$  mixtures in the corresponding region of the phase diagram [30] [31] and in some organic materials [32]. This should be contrasted with the low temperature ordered phases and the phase transitions into these ordered states which depend on the detailed orbital structure of the material [33][26].

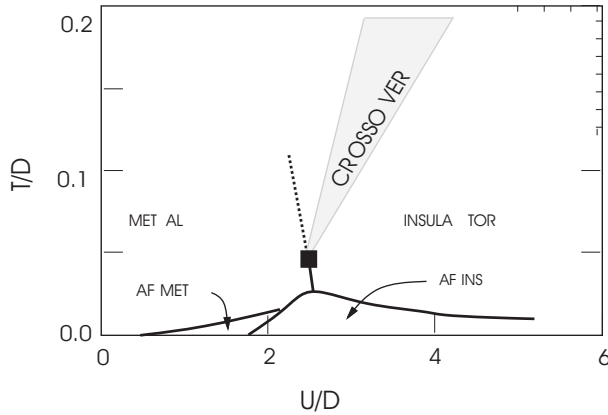


Figure 1.2: Schematic phase diagram of partially frustrated Hubbard model from Ref. [29]. The square dot denotes  $T_c U_c$ , the critical endpoint of the first order line. The dotted line continues the first order line above the second order endpoint. It denotes the location of the sudden rise of the resistivity shown in figure 1.3.

Notice the anomalously large metallic resistivity that is typical of many oxides [34]. While the curves in this figure far exceed the Ioffe-Regel limit (using estimates of  $k_f$  from  $T = 0$  calculations), there is no violation of any physical principle. At low temperatures, a  $\mathbf{k}$ -space based Fermi-liquid theory description works, but in this regime the resistivity is low (below the Ioffe-Regel limit). Above a certain temperature, the resistivity exceeds the Ioffe-Regel limit, and the quasiparticle description becomes inadequate. There is, however, no breakdown or singularities in our formalism. The spectral functions remain smooth; only the physical picture changes. At high temperatures, we have an incoherent regime in which the Ioffe-Regel criterion does not apply, because there are no long-lived excitations with well-defined crystal momentum in the spectra. The electron is strongly scattered, and is better described in real space. In this regime, there is no simple description in terms of  $\mathbf{k}$ -space elementary excitations, but one can construct a simple description and perform quantitative calculations if one uses a theory based on the spectral function as a fundamental object. The temperature dependence of the transport in the high-temperature, incoherent regime depends on whether the system is at integer-filling or doped, as may be seen from the analysis in Ref. [35].

Another manifestation of the interplay of itineracy and localization is the anomalous transfer of spectral weight observed in the one-electron spectrum and in the optical spectra of correlated systems, as the doping concentration or pressure is varied. When one proceeds from a metallic state to an insulating state one expects spectral weight to be removed from the low frequencies region. What is anomalous and unexpected is that this spectral weight reappears at much higher

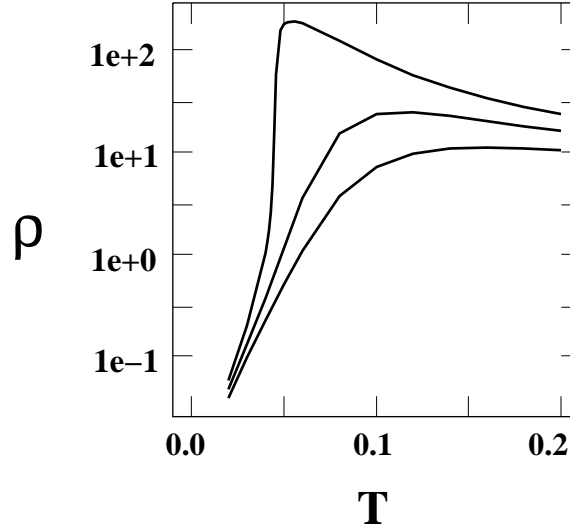


Figure 1.3: Resistivity  $\rho_{dc}(T)$  versus  $T$  above the critical endpoint of the line of first order phase transitions in figure 1.2.  $U/D = 2.1, 2.3, 2.5$  from bottom to top. From Ref. [29].

frequencies (of the order of  $U$  or  $D$ ) which is very different from what is observed in weak coupling superconducting of spin density wave systems. In weak coupling situations, when a small gap opens in the single particle spectra, the lost spectral density reappears in the immediate vicinity of the gap.

This surprising aspect of strong correlation physics was noted and emphasized by many authors [37]. Transfer of spectral weight can also take place as a function of temperature. For example, the ‘kinetic energy’ that appears in the low-energy optical sum-rule can have sizeable temperature dependence, an effect that was discovered experimentally [38], and explained theoretically by DMFT calculations [39].

Once again, thinking about this problem in terms of well-defined quasiparticles is not useful in this finite-temperature, strongly-correlated region. It is more fruitful to formulate the problem in terms of spectral functions describing, on the same footing, coherent and incoherent excitations.

The relative weights of the coherent and incoherent components of the spectra evolve rapidly with temperature, and lead to sizeable variations in the integrated optical intensity. The rapid variation of the low energy photoemission and optical spectral weight was predicted by the theory has already been seen in the  $V_2O_3$  and the  $NiSe_{2-x}S_x$  system [29][31] [41] [42]. These effects are most pronounced near the Mott transition endpoint, as shown in figure (1.5). Finally, the fundamental role of the spectral function becomes even more prominent in the Landau-theory approach to the Mott transition discussed in the next section in which

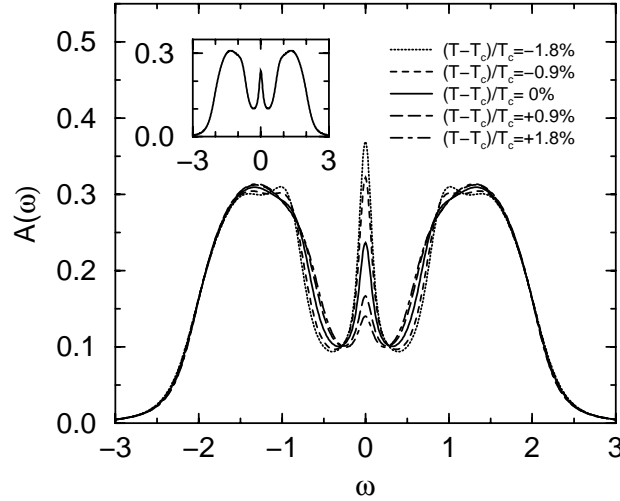


Figure 1.4: Evolution of the spectral function as function of temperature (bottom to top), near the finite temperature from Ref. [36]. The inset is the spectral function at the second order Mott endpoint.

the Greens function is allowed to fluctuate away from its physical saddle-point value to explore non-perturbative states that may not be accessed in a perturbation calculation in the interaction strength.

### 1.6 THE MOTT TRANSITION AS A BIFURCATION

A new perspective on the Mott transition is obtained by viewing the dynamical mean-field equations as a saddle-point of a Landau Ginzburg like functional [40], viz.

$$F_{LG}[\Delta] = -T \sum_{\omega} \frac{\Delta(i\omega)^2}{t^2} + F_{imp}[\Delta], \quad (1.22)$$

where

$$-\beta F_{imp} = \int df^+ df e^{-L_{loc}[f^+, f] - \sum_{\omega, \sigma} f^+_{\sigma}(i\omega) \Delta(i\omega) f_{\sigma}(i\omega)} \quad (1.23)$$

and  $L_{loc}[f^+, f] = \int_0^{\beta} f^+ [\frac{d}{d\tau} + \varepsilon_f] f + U f^+_{\uparrow} f_{\uparrow} f^+_{\downarrow} f_{\downarrow}$ . This functional may be understood by analogy with the Hubbard-Stratonovich construction of the free energy of the Ising model which in the absence of an external magnetic field is

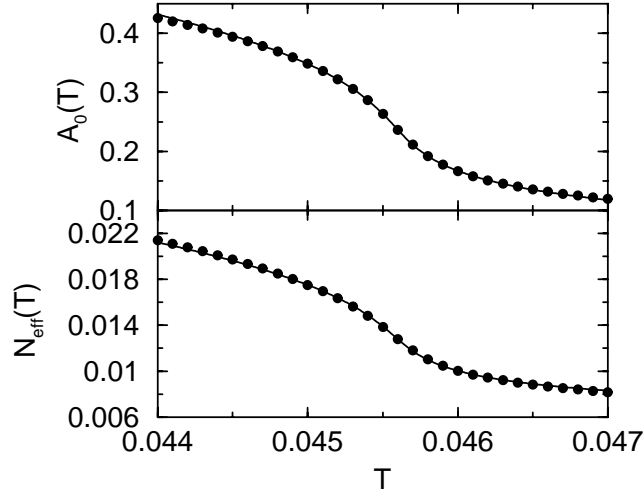


Figure 1.5: Integrated optical spectral weight  $N_{eff}$ , and quasiparticle weight,  $A_0$ , as function of temperature for  $U$  near  $U_c$

given by

$$\beta F_{LG}[h] = \beta \frac{h^2}{2Jz} - \log[\coth[\beta h]]. \quad (1.24)$$

The first term in Eqs. 1.22 and 1.24 represents the energy cost of forming the Weiss field, while the second term is the energy gain of the local degree of freedom (spin or electron in the classical and quantum cases, respectively). in the presence of the Weiss field. Differentiating eq. 1.24 gives the mean field theory described by eqs. (1.6) and (1.7).

A critical insight in this problem is the fact that the Mott transition point appears as a bifurcation point in the Landau functional (1.22). Even in infinite dimensions, we already know of several different classes of bifurcations, depending on whether we are at finite or zero temperature, and whether the transition takes place in the presence of magnetic long-range order. Zero-temperature bifurcation points are discussed in Ref. [40]. The bifurcation that takes place at the finite temperature endpoint of the line of first order phase transitions in figure 1.2,  $U_c T_c$ , was understood only very recently [36]. It is a simple Ising-like bifurcation, characterized by the fact that the fluctuation matrix

$$M_{nm} = \frac{t^2}{2T} \frac{\delta^2 F_{LG}[\Delta]}{\delta \Delta(i\omega_n) \delta \Delta(i\omega_m)} \Big|_{\text{critical point}} \quad (1.25)$$

acquires a single zero-energy mode  $\phi_0(i\omega_n)$ . The form of the critical theory is

derived by expanding around the critical point  $\alpha_c = (U_c, T_c)$  up to third order in the deviation of the hybridization function from its value at the critical point,  $\delta\Delta = \Delta(\alpha_c + \delta\alpha) - \Delta(\alpha_c)$ , and to first order in  $\delta\alpha = (U - U_c, T - T_c)$ . This expansion is well-behaved because the impurity model depends smoothly on  $\alpha$  and  $\Delta(i\omega_n)$ . The singular part of the component of the spectral function along the zero-energy mode is denoted by  $\eta$ , and plays the role of the order parameter of the finite temperature Mott transition endpoint. It obeys the equation [36]

$$c_1\eta + c_2\eta^3 = h. \quad (1.26)$$

Here  $c_1$  and  $c_2$  are smooth variables of  $U$  and  $T$ , which model pressure and temperature in the real physical systems.  $c_1$  at the endpoint of the first order Mott transition line, while  $c_2$  is non vanishing.

Since  $\delta\Delta \sim \eta\phi_0(i\omega_n)$ , the quantity  $\eta$  may be regarded as the *singular* part of the spectral function. It is observable in photoemission and inverse photoemission experiments. Almost all experimental probes, optical conductivity, transport coefficients etc., couple directly to the order parameter. Therefore, all these physical quantities should have an Ising-like singularity, which is generically driven by a magnetic field-like Ising variable with  $T - T_c$  or  $p - p_c$  (here,  $p$  is pressure) playing the role of the Ising model magnetic field. There is also a special combination of pressure and temperature which plays the role of an Ising-model temperature-like variable. Therefore, we expect near criticality  $\eta \approx (\delta\alpha)^{\frac{1}{\delta}}$ . In mean field  $\delta = 3$ , whereas  $\delta = 5, 15$  in three and two dimensions, respectively. However, the critical region of the finite-temperature Mott transition might be fairly small if, as in BCS theory, the coherence length for the fluctuation quantity  $\eta$  is inversely proportional to a power of  $T_c/\epsilon_F$ . The predictions of an Ising-like transition should be tested against careful experiments near the critical region of the compounds  $V_2O_3$  and  $NiSe_{2-x}S_x$ , or in other systems exhibiting a finite-temperature Mott endpoint to refine our understanding of the anomalous transfer of spectral weight discussed in the previous section.

The analysis of Ref. [36] reconciles two very different viewpoints on the Mott transition. Ideas put forward by Castellani *et al.* [43], in which the Mott transition appears as a condensation of doubly-occupied sites, are tied to a dual picture in which the Mott transition is associated with a rapid variation of the low energy part of the one-electron spectral function, as described in slave-boson, mean-field-theories [44].

An important quantity that generically couples to the order parameter  $\eta$  is the density,  $\delta n \approx a\eta \approx a\delta\mu^{\frac{1}{\delta}}$ . This dependence leads to a compressibility that diverges as

$$\frac{\delta n}{\delta\mu} = \delta\mu^{1-\frac{1}{\delta}} \approx \frac{1}{\delta n^{\delta-1}}. \quad (1.27)$$

Notice, however, that in particle-hole symmetric situations the coefficient  $a$  is

zero. The divergence in the compressibility can be observed at the second order endpoint of the chemical potential-driven Mott transition. It can also be observed at the endpoints of the interaction driven Mott transition for integer fillings which do not correspond to half filled shells. The compressibility is not singular in interaction driven Mott transition in the one band half filled Hubbard model because of its perfect particle hole symmetry.

The Landau functional in Eq. 1.22, viewed as a functional of the Weiss field or as a functional of the local Greens function, has several interesting properties. Its stationary point gives the physical Greens function and consideration of its bifurcations give interesting insights into the corresponding Mott transitions.

Generalizations of this construction to finite dimensions are highly desirable, and some progress was recently made by R. Chitra and the author [45]. A simple consequence of viewing the Mott transition as a smooth bifurcation is the connection between the Mott transition, viewed as a bifurcation in the one-electron Greens function (a one particle property), and the divergence of the compressibility (a two-particle property). This is interesting in light of the important work of Furukawa and Imada [46] who discovered that the approach to the Mott transition in two dimensions, as a function of doping, is characterized by a *divergence* of the charge susceptibility. Reference [45] proceeds by constructing a functional  $\Gamma$  of the one-electron Greens function that is stationary at the correct greens function. The Mott transition is a bifurcation of the stationary solutions of  $\delta\Gamma[G, \alpha]/\delta G = 0$ , as a control parameter  $\alpha$  is varied ( $\alpha$  may represent  $\mu$ ,  $T$  or  $U$ ). For a smooth bifurcation to take place at a critical value of the control parameter,  $\alpha_c$ , the matrix  $\chi = \frac{\delta^2\Gamma}{\delta G(x,y)\delta G(u,v)}$  has to be non invertible when evaluated at  $\alpha_c$ , since otherwise the equation

$$\delta G = - \left( \frac{\delta^2\Gamma}{\delta G \delta G} \right)_{\alpha_c}^{-1} \left( \frac{\delta^2\Gamma}{\delta G \delta \alpha} \right)_{\alpha_c} \delta \alpha \quad (1.28)$$

would have a unique solution for  $\delta\alpha + \alpha_c$ . This would contradict the starting assumption of a bifurcation point at  $\alpha_c$ . The smoothness assumption is crucial for this argument. In infinite dimensions at zero temperature, the necessary smoothness conditions are not satisfied. As a result, the compressibility vanishes at  $U_{c2}$  and remains finite when the Mott transition is approached as a function of chemical potential at  $\mu_{c2}$  [47]. The results in Ref. [46] and the previous arguments support the conjecture of Ref. [40] that the zero-temperature Mott transition in finite dimensions is smoother than its infinite-dimensional counterpart at  $T = 0$  and  $U = U_{c2}$ , perhaps closer in spirit to what was found at bifurcation point at the top of the coexistence region of the DMFT phase diagram (1.2) i.e. at  $U_c, T_c$ .

The finite-temperature Mott transition is really a transition between a ‘good’ and a ‘bad’ metal. The Landau analysis, which is based on an order-parameter description, is applicable to other localization-delocalization electronic transitions, such as the  $\alpha$ -to- $\gamma$  transition observed in the lanthanide series, and related transitions observed in some actinides[48]. To describe the  $f$  electrons in Ce,

we adopt the Anderson lattice model [48], which introduces, in the describes hybridization with a broad  $s - d$  band. Within the Anderson lattice Hamiltonian, one may prove that the first-order phase-transition line shown in Fig. 1.2 persists if the hybridization term is sufficiently small. This is a direct consequence of the smoothness of the Landau functional at finite  $T$ .

The Landau analysis demonstrates that the introduction of particle-hole asymmetry is a very relevant perturbation. Hence, it must be introduced as an essential ingredient in a model of  $f$  electrons such as Ce. Quantitative estimates of the phase diagram and the physical properties of the  $\alpha$ -to- $\gamma$  transition [49] requires a combination of realistic DMFT (as described in Ref. [50]) and explicit coupling of the DMFT energy to the lattice displacements (as in Ref. [51]). Nonetheless, we can already make exact statements about the critical behavior based on the Landau theory approach. For example, we predict an Ising-like divergence in the specific heat and in the bulk modulus (compressibility) of Ce at the finite-temperature endpoint of the  $\alpha$ -to- $\gamma$  transition line.

### 1.7 EXTENSIONS OF DYNAMICAL MEAN FIELD METHODS

The dynamical mean-field approach may be extended in several directions with a view towards realistic applications. To account for spin-spin and charge-charge interactions that are non-local, an extended dynamical mean-field approach (EDMFT) can be used [52] [53]. An imaginary time formulation starts from the action

$$\sum_{ij} \int \int d\tau d\nu c_{i\sigma}^+(\tau) F^{-1}(\tau i, \nu j) c_{\sigma j}(\nu) + \phi_{i\sigma}(\tau) B_{\sigma}^{-1}(\tau i, \nu j) \phi_{j\sigma}(\nu) \quad (1.29)$$

$$+ \sum_i \int d\tau U n_{i\uparrow} n_{i\downarrow} + \phi_{i\sigma}(\tau) n_{\sigma}(\tau).$$

This action describes a Fermion system interacting with a Bose field. The bare Bose and Fermi propagators are represented by  $B_{\sigma}^{-1}(\tau i, \nu j)$  and  $F^{-1}(\tau i, \nu j)$ , respectively. The case of long-range Coulomb interaction, corresponding to the addition of a term  $\sum_{i \neq j, \sigma \sigma'} V_{ij} : n_{i\sigma} n_{j\sigma'} :$ , was considered in Ref. [54] [this case corresponds to  $B_{\sigma}(q, i\omega_n) = V(q)$  in Eq. 1.29]. It produces qualitatively new effects, driving the Mott transition first-order even at zero temperature, where the conventional DMFT predicts a second order transition [55]. DMFT treats both electrons and the collective excitations (spin and charge fluctuations) on equal footing. The fermion (boson) propagators  $G$  and  $\Pi_{\sigma}$  are expressed in terms of the self-energies  $\Sigma(i\omega_n)$ , and  $\tilde{\Pi}_{\sigma}(i\omega_n)$ , which are assumed to be momentum independent, viz.

$$G^{-1}(i\omega_n, q) = i\omega_n - \epsilon_q - \Sigma(i\omega_n),$$

$$-\Pi_\sigma(q, i\omega_n) = \tilde{\Pi}_\sigma - B_\sigma^{-1}(q, i\omega_n).$$

The self-energies  $\tilde{\Pi}$  and  $\Sigma$  as well as other local quantities are computed from the local action

$$S_{loc} = \int d\tau d\tau' \sum_\sigma c_\sigma^+(\tau) \mathcal{G}_{0\sigma}^{-1}(\tau - \tau') c_\sigma(\tau') + \frac{U}{\beta} n_\uparrow(\tau) n_\downarrow(\tau) \delta(\tau - \tau') - \sum_\sigma \phi_\sigma(\tau) \Pi_{0\sigma}^{-1}(\tau - \tau') \phi_\sigma(\tau'). \quad (1.30)$$

The parameters of the local action are determined by solving the EDMFT self-consistency conditions which in the spinless case read:

$$\Pi_0^{-1}(i\omega_n) = \left[ \sum_q \frac{1}{-\tilde{\Pi}^{-1}\{\Pi_0, \mathcal{G}_0\}(i\omega_n) + B(q, i\omega_n)} \right]^{-1} + \tilde{\Pi}^{-1}\{\Pi_0, \mathcal{G}_0\}(i\omega_n), \quad (1.31)$$

and

$$\mathcal{G}_0^{-1}(i\omega_n) = \left[ \sum_q \frac{1}{i\omega_n - \epsilon_q - \Sigma\{\Pi_0, \mathcal{G}_0\}} \right]^{-1} + \Sigma\{\Pi_0, \mathcal{G}_0\}(i\omega_n). \quad (1.32)$$

A full solution of extended dynamical mean-field equations [53] for a spinless electron-phonon system, using the Quantum Monte-Carlo method, was obtained recently [56].

A second generalization is needed to deal with the electronic structure problem which starts with the atomic positions and the unit cell, but no *a priori* model Hamiltonian. It has been noted, by analogy with the Legendre transform construction of Density Functional Theory [57], that one may construct formally a functional of the local one-electron Greens function, which is stationary at the physical local spectral function. This construction was carried out to all orders in the interaction and was given a concrete diagrammatic interpretation [58], but is not unique since there are several possible definitions of what is meant by the local Greens function in the solid. In this approach DMFT is viewed as an exact theory.

While the density functional theory in the local approximation is closely related to the idea that the solid can be viewed as a perturbation around the homogeneous electron gas, Dynamical Mean-Field Theory, based on the concept of a Weiss field, offers a complementary perspective: The possibility of viewing the solid as a perturbation around a periodic collection of atoms. Formal developments of these ideas, combined with state-of-the-art electronic calculations,

are now producing first-principles calculations on materials for which density-functional calculations were unsuccessful (e.g.  $\delta$  plutonium [60]). Viewed from this perspective, the Mott transition problem has proved to be a valuable training ground for developing techniques for calculating electronic structure. These new methods handle the dual nature of the electrons (itinerant and localized) in a unified framework. A full-fledged realistic dynamical mean-field theory, including orbital degeneracy and band structure, is a new research tool in the science of complex materials with many possible applications.

An alternative approach focuses on functionals of the full one-electron particle, or its conjugate field as generalizations of the functional, and view dynamical mean-field as an approximate solution to the quantum many-body problem. In this view DMFT is an approximate theory. For example, the functional of the one-particle Greens function [45]

$$\Gamma[G] = -\text{Tr} \log[G_0^{-1} - \frac{\delta\Phi}{\delta G}] - \text{Tr} G \frac{\delta\Phi}{\delta G} + \Phi,$$

gives the dynamical mean-field equations when restricted to local Greens functions. Here,  $\Phi[G]$  is defined as the sum of all two-particle irreducible graphs computed with the full propagator  $G$ .

A third generalization involves extensions of DMFT to clusters [3]. Conceptually, the simplest generalization consists of dividing the lattice into supercells, and viewing each supercell as a complex ‘site’ to which one can apply ordinary DMFT. Denoting by  $R_n$  the supercell position and by  $\rho$  and  $\varsigma$  the sites within the unit cell, one may rewrite the kinetic energy term of the Hamiltonian in Eq. 1.1 in terms of a matrix  $\hat{t}_{\rho\varsigma}(\mathbf{k})$ , where  $\mathbf{k}$  is now a vector in the Brillouin zone (reduced by the size of the cluster due to the supercell construction). The local term in Eq. (1.1) is left unchanged. In supercell notation, the Hamiltonian reads

$$H = - \sum_{\rho\varsigma\sigma} \hat{t}_{\rho\varsigma}(k) c_{\rho\sigma}^+(k) c_{\varsigma\sigma}(k) + U \sum_{n\rho} n_{R_n\rho\uparrow} n_{R_n\rho\downarrow}. \quad (1.33)$$

The DMFT equations now become matrix equations relating the cavity Greens function  $\hat{G}_0$  and the self-energy matrix  $\hat{\Sigma}$  (both matrices are indexed by the cluster sites):

$$\hat{G}_0^{-1} = [\sum_k [i\omega - \hat{t}(k) - \hat{\Sigma}]]^{-1} + \hat{\Sigma}.$$

In the presence of long-range order, the supercell scheme reduces to the ordinary DMFT if in addition we ignore the intersite self energies. In the absence of long-range order, it contains additional information on short-range order.

The division of the lattice into supercells is artificial when spatial symmetries are not broken. Jarrell [59] and collaborators have suggested an alternative cluster scheme (the dynamic cluster approximation or DCA) to take into account the

lattice periodicity. That approach relies on clusters with periodic boundary conditions. Lichtenstein and Katsenelson [61] have applied cluster methods together with an interpolation scheme in  $k$  space to produce continuous self energies. The interplay of superconductivity and antiferromagnetism is currently being studied with these periodic cluster methods [61] [62].

## 1.8 CONCLUSIONS

Dynamical mean-field methods provide a zeroth-order starting point for describing the strongly correlated regime of many three-dimensional transition-metal oxides. Further generalizations, as the ones mentioned in this section and related schemes, are likely to be useful for attacking the major open problem in this field, how to incorporate the effects of magnetic correlations (with no magnetic long-range-order) in the theory of the Mott transition.

From a broader perspective, we have simple physical pictures as well as powerful computational tools to understand complex materials containing  $f$  and  $d$  electrons. The future of the theory of strongly correlated electrons, a field which Phil Anderson pioneered with his unique depth creativity and insight seems very bright and will continue to thrive in this new century.

## BIBLIOGRAPHY

- [1] N. F. Mott, *Proc. Roy. Soc. A* **62** 416 (1949).
- [2] For a recent review and for further references see M. Imada, A. Fujimori, and Y. Tokura, *Rev. Mod. Phys.* **70** 1039 (1998).
- [3] For a recent review and further references, see A. Georges, G. Kotliar, W. Krauth, and M. Rozenberg, *Rev. Mod. Phys.* **68** 13 (1996).
- [4] P. W. Anderson, *Phys. Rev. B* **115** 2 (1959).
- [5] Hubbard, J., *Proc. Roy. Soc. (London)* **A281**, 401, (1964).
- [6] for a review see the *Mathematics and Physics of the Hubbard model*. D. Bareswyl et. al Editors, Plenum Press, New York. (1995)
- [7] W. Metzner and D. Vollhardt, *Phys. Rev. Lett.* **62** 324 (1989).
- [8] Müller-Hartmann, E., *Z Phys. B* **74**, 507, (1989). 237.
- [9] Müller-Hartmann, E., *Z. Phys. B* **76**, 211, (1989).
- [10] F. Gebhardt *Phys. Rev. B* **41** , 9452 (1990) and **44** 992 (1991)
- [11] Brandt, U. and C. Mielsch, *Z. Phys.* **75**, 365 (1989).

- [12] P. W. Anderson, *Phys. Rev.* **124** 41 (1969).
- [13] A. Georges and G. Kotliar, *Phys. Rev. B* **15** 6479 (1992).
- [14] Kuramoto, Y. and T. Watanabe, *Physica* **148B**, (1987). Ohkawa, F. J., *J.Phys.Soc.Jpn* **60**, 3218 (1991). Janiš, V., *Z. Phys. B* **83**, 227, (1991). [3] Jarrell, M., *Phys. Rev. Lett.* **69**, 168 (1992).
- [15] Kotliar, G., in "*Strongly Correlated Electronic Materials*", K. Bedell, Z. Wang, D. Meltzer, A. Balatzky, E. Abrahams eds, (Adison-Wesley) (1993).
- [16] A. Hewson, *The Kondo Problem, Cambridge Studies in Magnetism Vol 2.* Cambridge University Press Cambridge England (1993).
- [17] P. W. Anderson and G. Yuval, *Phys. Rev. Lett.* **23** 89 (1969); P. W. Anderson, G. Yuval, and D. Hamman, *Phys. Rev. B* **1** 4464 (1970).
- [18] Hirsch, J. E. and Fye, R. M., *Phys. Rev. Lett.* **56**, 2521 (1986).
- [19] Rozenberg, M., X. Y. Zhang and G. Kotliar, 1992, *Phys. Rev. Lett.* **69**, 1236 (1992). Georges, A., and W. Krauth, , *Phys. Rev. Lett.* **69**, 1240 (1992).
- [20] X. Y. Zhang, M. Rozenberg, and G. Kotliar, *Phys. Rev. Lett.* **70** 1666 (1993).
- [21] A. Fujimori *et al.*, *Phys. Rev. Lett.* **69** 1796 (1992).
- [22] F.D.M. Haldane *J. Phys. C* **11** 5015 (1978).
- [23] Q. Si G. Kotliar and A. Georges *Phys. Rev. B* **46**, 1261 (1992).
- [24] Q. Si and G. Kotliar *Phys. Rev. Lett* **70** 3143 (1993)
- [25] L.M. Falikov and J. C. Kimball , *Phys. Rev. Lett* **22**, 997 (1969)
- [26] R. Chitra and G. Kotliar, *Phys. Rev. Lett* **83**, 2386 (1999).
- [27] H. Kajueter and G. Kotliar, *Int. J. Mod. Phys.* **11** 729 (1997).
- [28] A. Georges and W. Krauth, *Phys. Rev. B* **48** 7167 (1993).
- [29] M. Rozenberg, G. Kotliar, and X. Y. Zhang, *Phys Rev. B* **49** 10181 (1994); M. Rozenberg *et al.*, *Phys. Rev. Lett.* **75** 105 (1995).
- [30] Mc Whan D. B. Remeika J. Brinkman W. and Rice T. M. *Phys. Rev. B* **7**, 1920 (1973). Kuwamoto H. Honig J. and Appel J. *Phys. Rev. B* **22** 2626 (1980)
- [31] A. Miyasaka and H. Takagi unpublished.

- [32] H. Ito et. al. J. Phys. Soc. Jpn **65**, 2987 (1996). K. Kanoda Physica C, 282-287, 299 (1987).
- [33] G. Kotliar Physica B, **259-261** (1999) 711.
- [34] V. J. Emery and S. Kivelson, Phys. Rev. Lett. **74** 3253 (1995).
- [35] G. Palsson and G. Kotliar, Phys. Rev. Lett. **80** 4775 (1998).
- [36] G. Kotliar, E. Lange, and M. Rozenberg, Phys. Rev. Lett. **84**, 5180-5183 (2000).
- [37] For an early discussion, see H. Eskes, M. B. J. Meinders, and G. A. Sawatzky Phys. Rev. Lett. **67** 1035 (1991).
- [38] Z. Schlesinger **et al.**, Phys. Rev. Lett. **71** 1748 (1993).
- [39] M. Rozenberg, G. Kotliar, and H. Kajueter, Phys. Rev. B **54** 8452 (1996).
- [40] G. Kotliar, Euro. J. Phys. B, **11** 27 (1999).
- [41] A. Matsuura et. al. Phys. Rev. B **58**, pp. 3690-3696 (1998).
- [42] S. Watanabe and S. Doniach Phys. Rev. B **58**, pp. 3690 (1998).
- [43] C. Castellani, C. D. Castro, D. Feinberg, and J. Ranninger, Phys. Rev. Lett. **43** 1957 (1979).
- [44] G. Kotliar and A. Ruckenstein, Phys. Rev. Lett. **57** 1362 (1986).
- [45] R. Chitra and G. Kotliar, cond-mat/9911223.
- [46] N. Furukawa and M. Imada, J. Phys. Soc. Jpn. **61** 331 (1992); **62** 2557 (1993).
- [47] H. Kajueter, G. Kotliar, and G. Moeller, Phys. Rev. B **53** 16214 (1996).
- [48] A. Mc. Mahan *et al.*, J. Comput-Aided Mater. Des. **5** 131 (1998).
- [49] J. W. Allen and R. M. Martin Phys. Rev. Lett **49**, 1106 (1982). L. Z. Liu et. al. Phys. Rev. B **45**, 8934 (1992).
- [50] V. Anisimov *et al.*, J. Phys. Cond. Matt. **9** 7359 (1997).
- [51] P. Majumdar and H. R. Krishnamurthy, Phys. Rev. Lett. **73** 1525 (1994).
- [52] S. Sachdev and Y. Ye Phys. Rev. Lett. **70**, 339, (1993).
- [53] Q. Si and J. L. Smith, Phys. Rev. Lett. **77** 3391 (1997); H. Kajueter, Rutgers University Ph.D. Thesis, (1996).

- [54] R. Chitra and G. Kotliar, Phys. Rev. Lett 84, 3678-3681 (2000).
- [55] G. Moeller, Q. Si, G. Kotliar, M. Rozenberg and D. S Fisher, Phys. Rev. Lett. **74**, 2082 (1995).
- [56] Y. Motome and G. Kotliar, submitted to Phys. Rev. B.
- [57] M. Valiev and G. Fernando, Phys. Lett. A **227** 265 (1997).
- [58] R. Chitra and G. Kotliar, cond-mat/9911056.
- [59] C. Huscroft *et al.*, cond-mat/9910226;  
Maier T, Jarrell M, Pruschke T, Keller J.Eur.Phys. Jour. **B 13** 2000, 613.  
Hettler M.H., et. al. Phys. Rev **.B 58** (1998) 7475.
- [60] S. Savrasov and G. Kotliar, Phys. Rev. Lett. 84, 3670-3673, (2000).
- [61] L Lichtenstein and M. Katsenelson cond-mat/9911320. Phys. Rev. B in press.
- [62] Th. Maier, M. Jarrell, Th. Pruschke, J. Keller cond-mat/0002352